JOURNAL OF MATERIALS SCIENCE 18 (1983) 2319–2336

# A fracture mechanics analysis of polypropylene/rubber blends

J. M. HODGKINSON, A. SAVADORI,* J. G. WILLIAMS
*Department of Mechanical Engineering, Imperial College of Science and Technology, Exhibition Road, London, SW7 2BX, UK*

The results of previous work, in which static fracture tests were applied to propylene–ethylene copolymers, suggest that under circumstances of high constraint the theory of fracture mechanics is useful in the description of the fracture behaviour of such tough materials. In this work similar experiments have been carried out on a series of polypropylene/EPR/HDPE blends in order to compare their behaviour with that of the copolymers. From the evidence it appears that these materials are very similar to the copolymers in terms of fracture behaviour and morphology. The examination of impact fracture behaviour of the blends showed that both instrumented and energy measuring pendulum machines yield similar results when loading times are similar. However, it has been shown that short loading times may lead to high fracture energies, which cause blunting of the crack tip. This behaviour has been modelled using previously developed theory. The effects described demonstrate the care required in impact data interpretation.

## Nomenclature

| | |
|---|---|
| $a$ | crack length. |
| $b$ | notch width for surface notch specimen. |
| $B$ | specimen thickness. |
| $c$ | specific heat. |
| $D$ | specimen width. |
| $E$ | elastic modulus. |
| $E'$ | dynamic storage modulus. |
| $G_c$ | strain energy release rate. |
| $G_b$ | apparent strain energy release rate. |
| $k$ | thermal conductivity. |
| $K_c$ | critical stress intensity factor. |
| $K_{c1}$ | plane strain fracture toughness. |
| $K_{1c}$ | instability fracture toughness. |
| $K_c'$ | apparent toughness (SEN) |
| $K_{c2}$ | plane stress fracture toughness. |
| $L$ | specimen span in impact. |
| $M_w$ | weight average molecular weight. |
| $M_n$ | number average molecular weight. |
| $M_w/M_n$ | polydispersity ratio. |
| $N$ | notch blunting parameter. |
| $\tan\delta$ | loss factor. |
| $t$ | loading time in impact. |
| $t_1$ | limiting loading time. |
| $t_0$ | loading time for beginning of thermal blunting. |
| $T_0$ | test temperature. |
| $T_s$ | softening temperature. |
| $V$ | striker velocity in impact. |
| $w$ | impact fracture energy. |
| $w_k$ | kinetic energy. |
| $x$ | $a/D$. |
| $Y$ | finite width correction factor. |
| $\sigma_y$ | yield stress. |
| $\sigma_c$ | fracture stress. |
| $\phi$ | compliance function. |
| $\rho$ | density. |
| $[\eta]$ | limiting viscosity number. |

## 1. Introduction

It is well known and now widely accepted that linear elastic fracture mechanics forms a suitable framework for the discussion of fracture processes in such glassy polymers as polymethyl methacrylate and polystyrene. For such materials the plane

*On leave from Centro Ricerche Giulio Natta, Montepolimeri, S.p.A., Ferrara, Italy

0022–2461/83 $03.00 + .12 

strain fracture toughness $K_{c1}$ describes precisely the initiation of an unstable fracture process leading to catastrophic failure. What is not perhaps as widely held a view is that fracture mechanics theory may be extended to relatively tough materials which normally exhibit significant plasticity prior to fracture. It has, however, been shown [1–3] that several fracture testing techniques are suitable for use with such materials in the determination of toughness. In order to adhere to the requirement that the plastic zone be small, and hence to define a true plane strain toughness, experiments on those tougher materials have frequently been carried out at low temperatures or on large specimens to minimize plane stress effects. In addition to such static fracture toughness testing there has also been considerable activity in the field of high speed impact fracture of tough materials, and the application of fracture mechanics has proven successful here too [4]. In these tests the impact fracture toughness or strain energy release rate, $G_c$, was determined in the Charpy and Izod modes over wide ranges of temperature and strain rate.

Polypropylene homopolymer is not a tough material at low temperatures, but manufacturers have succeeded in copolymerizing it with ethylene to form a relatively tough two phase product. Polypropylene forms the matrix, and a rubber-like phase consisting of an ethylene–propylene copolymer acts as a toughening dispersed phase [5, 6]. It is also common to find physical blends of polypropylene homopolymer with a rubbery reinforcing component, having similar toughness properties to the equivalent copolymerized material.

Fernando and Williams [1] investigated the fracture behaviour of a polypropylene homopolymer and two copolymers of ethylene and propylene with a toughening dispersed phase. The brittle behaviour of these materials was characterized in terms of the instability fracture toughness $K_{1c}$, and the effects of specimen shape, notch sharpness and mode of loading, studied in order to determine the plane strain toughness $K_{c1}$. It was demonstrated that these materials could be discussed in terms of $K_{c1}$, determined in bending under high constraint to plastic flow at the crack tip, $K_c$, the apparent toughness determined in a single edge notch (SEN) tension, where there is little constraint, and the yield stress, $\sigma_y$. From the experimental evidence over a range of temperatures between +30 and −160° C it was concluded that the addition of ethylene caused increased ductility, suppressing the yield stress and the ductile–brittle transition temperature. The copolymers exhibited a ductile–brittle transition in the region −100 to −45° C, and were completely brittle below −100° C. Above −45° C it was found that some slow growth preceded unstable fracture, and above −30° C the copolymers were completely ductile. The homopolymer showed no evidence of these intermediate regions becoming ductile at about +30° C. Further work [2] on a series of copolymers of ethylene and propylene, with ethylene contents varying between 1 and 17%, showed that the yield stress decreased with increased ethylene content whilst yield strain remained fairly constant. Using SEN in three point bending, the plane strain fracture toughness $K_{c1}$ was determined at −60° C and was apparently independent of ethylene content after an initial drop from the value obtained for the homopolymer.

The two papers [1, 2] taken together provide a comprehensive study of the nature of brittle fracture behaviour in polypropylene homopolymer and its associated copolymers with ethylene. Although no equivalent study has been published on the fracture behaviour of blends of polypropylene with ethylene–propylene rubber (EPR), similar blends have been the subject of general property and impact testing. In particular Stehling *et al.* [7] studied blends of polypropylene with EPR and small amounts of high density polyethylene (HDPE). They carried out Izod and falling weight impact tests on notched and unnotched specimens and determined the flexural modulus using standard test methods. The morphology of the materials was studied using scanning electron microscopy coupled with an etching technique to dissolve the rubber revealing the polypropylene matrix. Changes in impact strength and modulus caused by blend composition were interpreted in terms of size, composition and structure of the dispersed rubbery phase. A further study of polypropylene blended with ethylene/propylene/diene terpolymer (EPDM) rubbers [8] used instrumented impact testing on blunt notched Charpy specimens and attempted, with some success, to correlate the impact strength, dynamic storage modulus $E'$ and loss factor $\tan\delta$ over a wide temperature range. In fact this type of correlation of toughness with loss peaks has been observed previously in other

materials with blunt notches [9] and also using sharp notches with a fracture mechanics analysis [10]. Whilst both papers [7, 8] seek to correlate blunt notch impact behaviour with physical properties and microstructure, neither was concerned with fracture mechanics, slow rate fracture tests or the definition of a minimum fracture toughness described by the plane strain value $K_{c1}$.

This present work is concerned with the properties of blends of polypropylene with ethylene–propylene rubber and HDPE. The static fracture tests used are similar to those of Fernando and Williams [1, 2] in an attempt to define the plane strain fracture toughness $K_{c1}$. In addition sharp notch impact tests at room temperature compare the results of an instrumented pendulum machine with those from an energy measuring pendulum. Dynamic mechanical tests and optical and electron microscopy reveal systematic changes due to blending.

## 2. Materials

The base materials from which the blends were made were a polypropylene homopolymer Moplen®, an ethylene–propylene rubber Dutral® and a high density polyethylene Moplen-RO®. These materials were fully characterized and their main physical and mechanical properties are indicated in Table I.

Blends were obtained from a master batch system by the following procedure.

(a) Master batch (A)

EPR + polypropylene
50% 50%
Banbury mixing
and pelletizer

→ (A) + polypropylene dry blending and extrusion → Blend 1.
90% polypropylene, 10% EPR.

→ Blend 2.
80% polypropylene, 20% EPR.

(b) Master batch (B)
EPR + HDPE
66% 34%
Banbury mixing
and pelletizer.

→ (B) + polypropylene dry blend and extrusion. → Blend 3.
85% polypropylene, 10% EPR, 5% HDPE

In addition to the three blends the homopolymer was also available. Some of the physical characteristics of the homopolymer and blends are shown in Table II. Further processing of the four materials was necessary in order to obtain plaques from which specimens could be cut for mechanical testing. Plaques were prepared by injection moulding and had overall dimensions 300 mm x 150 mm. The mould was side-gated, and specimens for fracture testing were machined from the plaques according to the dimensions shown in Fig. 1, taking care to machine similar specimens from the same area each time.

## 3. Experimental details

### 3.1. Static fracture tests

The test methods used for the slow rate fracture tests were similar to those described in detail by Fernando [1, 2, 11] with tests being made in single edge notch (SEN) tension and bending, and surface notch (SN) in bending. The specimen configurations for these tests are shown in Fig. 1. For the SEN tension tests at −40° C all materials except the homopolymer exhibited a ductile type of failure. Instead of the linear load/displacement curve, characteristic of brittle fracture, shown in Fig. 2a for the homopolymer, curves such as that shown in Fig. 2b were obtained. This ductile behaviour was evident from the failed material which showed a high degree of plastic yielding and through thickness contraction prior to fracture. Tests at −60° C gave ductile behaviour in the high rubber content blend 2 but all other materials at this temperature, and all materials at below −60° C behaved in a brittle manner. The behaviour in SEN bending proved to be almost identical to that in tension with blends becoming brittle at between −40 and −80° C. Surface notched specimens were tested in bending but only at −80° C, so that all fractures were of a brittle nature.

In each case the maximum load condition was used to calculate the gross stress $\sigma_c$ at fracture, and the critical stress intensity factor $K_c$ calculated from the relationship

TABLE I Physical characteristics of the base materials

| Characteristic | Polypropylene homopolymer | Ethylene/propylene rubber | HDPE |
|---|---|---|---|
| Melt flow rate | 3.3 g(10 min)$^{-1}$ 230° C(2.16 kg) | – | 6.0 g(10 min)$^{-1}$ 190° C(2.16 kg) |
| Mooney at 121° C ASTM D 1646 | – | 90 | – |
| $[\eta]$ | 1.9 dl g$^{-1}$ at 135° C in tetrahydronaphthalene | 3.0 dl g$^{-1}$ at 125° C in tetrahydronaphthalene | 1.2 dl g$^{-1}$ at 110° C in $\alpha$-chloronaphthalene |
| Wt % $C_3$ | – | 50% | – |
| $M_w \times 10^{-3}$ | 440 light scattering | 380 GPC | 180 light scattering |
| $M_w/M_n$ | 8.6 GPC | 4.3 GPC | 7.9 GPC |
| Density ASTM D1505 | 0.904 g cc$^{-1}$ | 0.855 g cc$^{-1}$ | 0.960 g cc$^{-1}$ |
| Tacticity index | 96% isotactic insoluble in boiling heptane | – | – |
| Crystallinity | 58% X-ray analysis | – | – |

$$K_c = \sigma_c Y(a)^{1/2}. \quad (1)$$

Here $Y$ is a geometric finite width correction factor which may be calculated for any shape of specimen [12] and $a$ is the crack length. An example of the results from SEN tests on the homopolymer at −60° C is shown in Fig. 3, where $\sigma Y$ is plotted against $a^{-1/2}$, the resulting slope giving the fracture toughness $K_c$. The results for the range of temperatures and materials tested are presented in Table III.

## 3.2. Impact fracture

The form of the impact test adopted here was the Charpy pendulum test where the specimen is effectively in three-point bending, as shown in Fig. 1, but two different machines were used. Sets of specimens were fractured at 3.46 m sec$^{-1}$ and 23° C using an energy measuring system which has been in use for some years [13]. Each batch consisted of a number of specimens with different notch lengths, the notch being a fly cut 60° Vee with a root radius 15 $\mu$m. It was possible, with this approach, to make use of the fracture mechanics analysis developed initially for brittle polymers [14] and extended later to more ductile materials [13]. In this analysis the strain energy release rate or impact fracture toughness, $G_c$, is related to fracture energy, specimen and notch dimensions and compliance by the equation:

$$w = G_c BD\phi + w_k \quad (2)$$

where $w$ is the fracture energy, $w_k$ the kinetic energy of the broken specimen halves, $BD$ is the cross-sectional area ($B$ was varied between 3 and 12 mm to allow investigation of the thickness effect) and $\phi$ the compliance calibration factor which is a function of specimen geometry and

TABLE II Physical characteristics of blends

| Characteristic | Method | Unit | Homopolymer | Blend 1 | Blend 2 | Blend 3 |
|---|---|---|---|---|---|---|
| Melt flow rate 230° C(2.16 kg) | ASTM D1238 | g(10 min)$^{-1}$ | 3.3 | 3.0 | 2.2 | 2.7 |
| Density | ASTM D1505 | g cc$^{-1}$ | 0.904 | 0.890 | 0.893 | 0.902 |
| Notched Izod 23° C | ASTM D256 | J m$^{-1}$ | 43 | 125 | 500 | 200 |

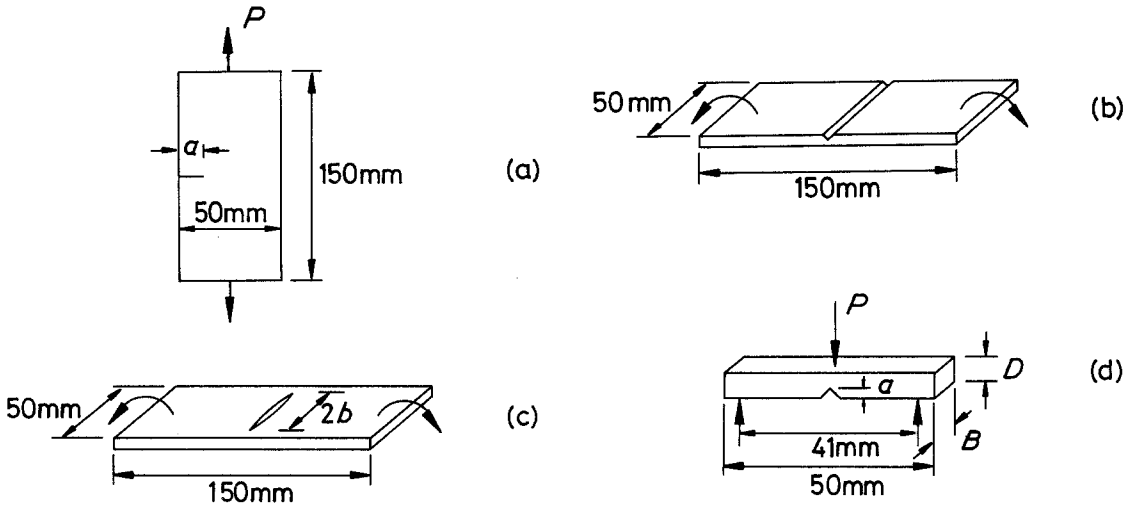


*Figure 1* Specimen configurations, (a) SEN tension, (b) SEN bending, (c) SN bending and (d) Charpy impact.

notch dimensions. From Equation 2 it can be seen that a plot of fracture energy against $BD\phi$ yields $G_c$ as the slope of the line described by the data, $w_k$ being indicated by the positive energy intercept of this line. An example of this type of analysis is shown in Fig. 4 for blend 1, and impact toughness values for the other materials are presented in Table IV.

In addition to the energy measuring impact test, further tests were carried out on an instrumented pendulum machine which has been used previously [15, 16] in the determination of toughness parameters. A Kistler-quartz piezoelectric transducer attached to the pendulum allowed recordings of load to be made on a Biomation model 805 waveform recorder. The apparatus has been described in detail elsewhere [15]. In order to avoid stress wave effects and resonances in the pendulum/transducer couple, it was necessary to reduce the striking velocity to $2\,m\,sec^{-1}$. Notches

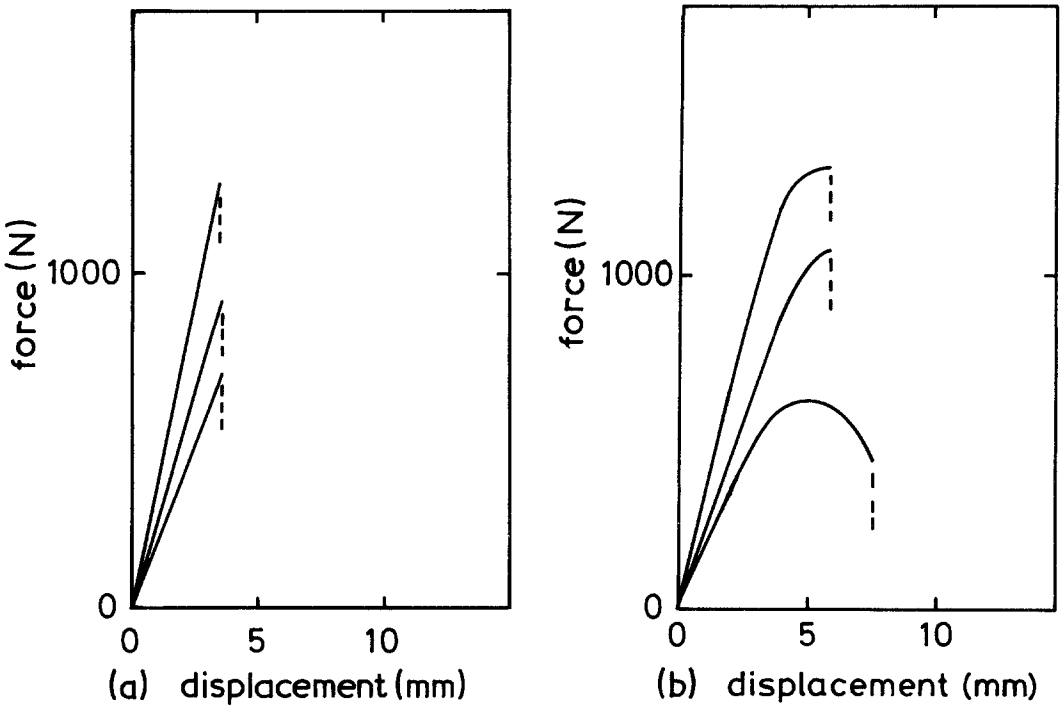


*Figure 2* SEN tension load displacement curves at −40° C, (a) homopolymer and (b) blend 1.

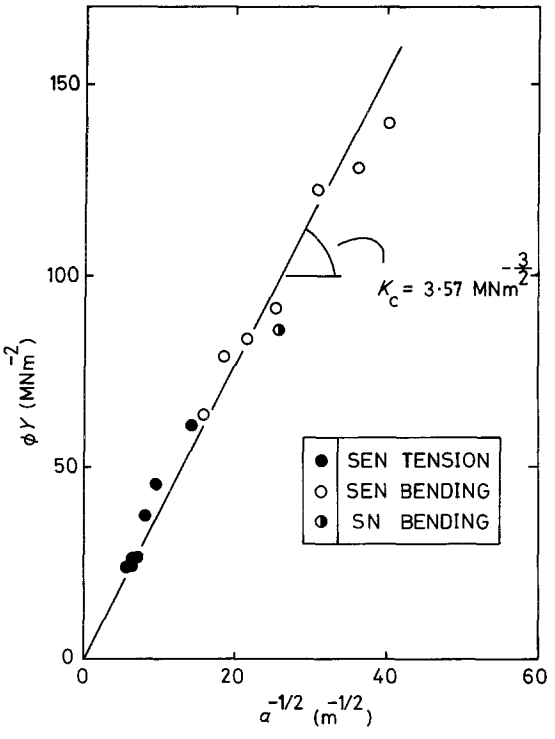


*Figure 3* Fracture toughness for polypropylene homopolymer at −60° C by several methods.

were made by razor blade, and $K_c$ determined by use of Equation 1. Specimen thickness was varied between 3 and 12 mm and the notch depth to width ratio ($a/D$) was also varied. Fig. 5 shows the load/time curves for the homopolymer and blend 1, the linearity of the ralationship for the homopolymer indicating the brittle behaviour of the material. Some curvature is noted for blend 1 however, and in Fig. 6 blends 2 and 3 indicate increased non-linear behaviour particularly at high $a/D$ ratios. These effects are discussed in detail below.

### 3.3. Dynamic mechanical properties

Measurements were made of dynamic modulus and tan δ by a resonance method carried out according to DIN 53440 at a frequency of 1000 Hz. The curves for dynamic modulus are shown in Fig. 7 and are much as expected. From what may be considered a plateau modulus below 0° C, an increase in temperature through the glass transition ($T_g$) produces a rapid decrease in stiffness. The homopolymer has the highest modulus throughout the whole temperature range, the addition of rubber resulting in a corresponding deterioration in stiffness, dependent upon the rubber volume fraction. For the same rubber content, a further addition of HDPE appears to have no significant effect since the curves for blends 1 and 3 are almost identical.

The loss factor curves of Fig. 7 indicate that the homopolymer has two peaks, a strong peak at +25° C and a relatively weak shoulder at −60° C. At temperatures above 0° C the blends follow the same curve as the homopolymer, but below 0° C a rapid divergence is noted. The shoulder which occurs at −60° C in the homopolymer is absorbed into a strong peak centred at −40° C for all the

TABLE III Static toughness data

| Material | Temperature (° C) | $K_{c_1}$ (MN m$^{-3/2}$) 3-point bending | $K'_c$(MN m$^{-3/2}$) SEN | $K_c$(MN m$^{-3/2}$) SN | $K_{c_2}$ (MN m$^{-3/2}$) |
|---|---|---|---|---|---|
| Homopolymer | −40 | 3.24 | – | – | – |
| Homopolymer | −60 | 3.57 | 3.57 | – | – |
| Blend 1 | | 3.30 | 5.07 | – | 6.90 |
| Blend 2 | | 2.97 | 5.94 | – | 6.79 |
| Blend 3 | | 3.20 | 4.99 | – | 6.87 |
| Homopolymer | −80 | 3.64 | – | 3.29 | – |
| Blend 1 | | 3.33 | 3.98 | 2.88 | 6.12 |
| Blend 2 | | 2.97 | 3.75 | 3.07 | 5.75 |
| Blend 3 | | 2.91 | 3.48 | 2.70 | 5.66 |
| Homopolymer | −100 | 3.88 | – | – | – |
| Blend 1 | | 3.35 | 3.70 | – | 5.70 |
| Blend 2 | | 2.86 | 3.20 | – | 5.20 |
| Blend 3 | | 3.49 | 3.71 | – | 5.30 |
| Homopolymer | −120 | 3.95 | – | – | – |
| Blend 1 | | 3.20 | – | – | 3.20 |
| Blend 2 | | 2.96 | – | – | 2.96 |
| Blend 3 | | 3.50 | – | – | 3.50 |

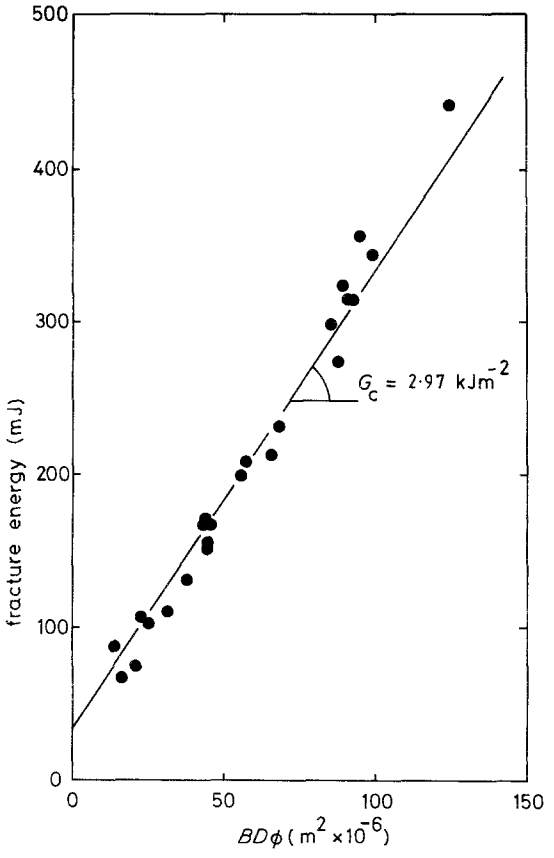


*Figure 4* Impact fracture energy as a function of $BD\phi$ for blend 1 (10% rubber) at +23° C, $B$ = 6 mm.

blends. The height of this peak is dependent upon rubber content and is likely to indicate the $T_g$ of EPR. There is however a small effect in blend 3 due to the addition of HDPE, the curve being in an intermediate position between blends 1 and 2 in the region −10 and −45° C. This may be interpreted as a contribution from the $\beta$ transition in HDPE [4] having an additive effect in this region. The blends also exhibit a further peak at around −100° C indicating $T_g$ for the polyethylene sequences of the rubber. With the addition of HDPE (blend 3) the centre of this peak moves to a slightly higher temperature, probably due to the decreased mobility of the free polyethylene chains, the peak height being almost equivalent to the 20% rubber blend 2.

## 4. Morphology

### 4.1. Optical microscopy

Sections 5 $\mu$m thick were microtomed for viewing on a Nikon Optiphot Universal microscope. The microscope was equipped with both a polarizing capability, and a technique known as differential interference contrast (DIC). DIC is a technique which is sensitive to microscopic variations in light paths of two beams generated by the Nomarski prism [17], so that small changes in specimen thickness or refractive index caused by the presence of separate phases may be identified [5]. Fig. 8a shows the homopolymer in transmitted DIC, and the spherulitic structure revealed is typical of polypropylene, and here the dimensions of the spherulites are typically 50 $\mu$m edge to edge. Fig. 8b shows the effect of 10% blended rubber, the technique used reveals the rubber as a dispersed second phase in the polypropylene matrix. This second phase takes the form of small round inclusions of between 1 and 2 $\mu$m in diameter. Although the spherulitic structure of the matrix is still visible, it is clearly being disguised by the presence of the rubber particles. When the amount of rubber blended is increased to 20% as shown in Fig. 8c, the size of the rubber

TABLE IV Impact toughness data at 23° C

| Material | Thickness $B$ (mm) | Impact toughness $G_c$ (kJ $m^{-2}$) | $K$ from $K_c^2 = EG_c$ (MN $m^{-3/2}$) | $K$ from Instrumented test (MN $m^{-3/2}$) | Dynamic modulus (GN $m^{-2}$) |
|---|---|---|---|---|---|
| Homopolymer | 3 | 1.20 | 1.65 | 1.65 | 2.28 |
| | 6 | 1.74 | 1.99 | 2.09 | |
| | 12 | 1.58 | 1.89 | 1.82 | |
| Blend 1 | 3 | 2.10 | 1.95 | 2.44 | 1.81 |
| | 6 | 2.97 | 2.32 | 2.59 | |
| | 12 | 2.90 | 2.29 | 2.59 | |
| Blend 2 | 3 | 4.00 | 2.40 | 2.70 | 1.44 |
| | 6 | 4.76 | 2.61 | 2.81 | |
| | 12 | 4.79 | 2.62 | 2.96 | |
| Blend 3 | 3 | 3.40 | 2.39 | 2.68 | 1.68 |
| | 6 | 3.92 | 2.56 | 3.00 | |
| | 12 | 3.71 | 2.49 | 3.00 | |

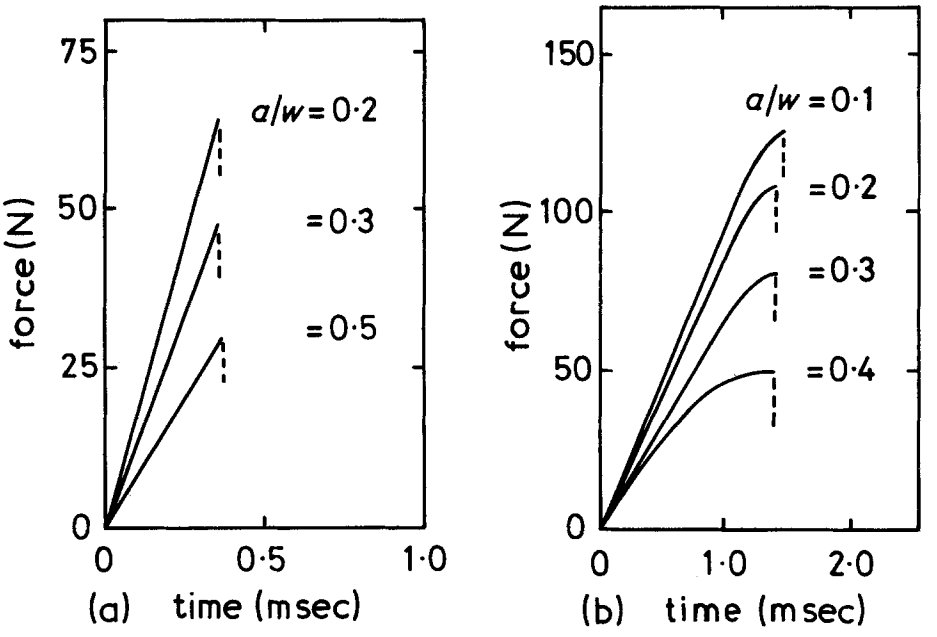


*Figure 5* Load–time curves from instrumented impact at +23° C, $B = 3$ mm, (a) homopolymer and (b) blend 1.

inclusions does not appear to increase, but their frequency does. The spherulites in this photomicrograph are now virtually indistinguishable. In Fig. 8d 10% rubber and 5% HDPE have been blended with the matrix, and in this case the spherulites are now completely obliterated by the included phase. The rubber particles are no longer as clearly defined as with the simple combinations of rubber and matrix.

The use of crossed polars also revealed the spherulitic structure of the polypropylene matrix, and as the rubber and HDPE were blended the spherulites were again gradually disguised and finally obliterated. In this approach however there was no evidence of a second phase being present, no rubber particles were visible, so that the technique was discarded as being unsuitable for this work.

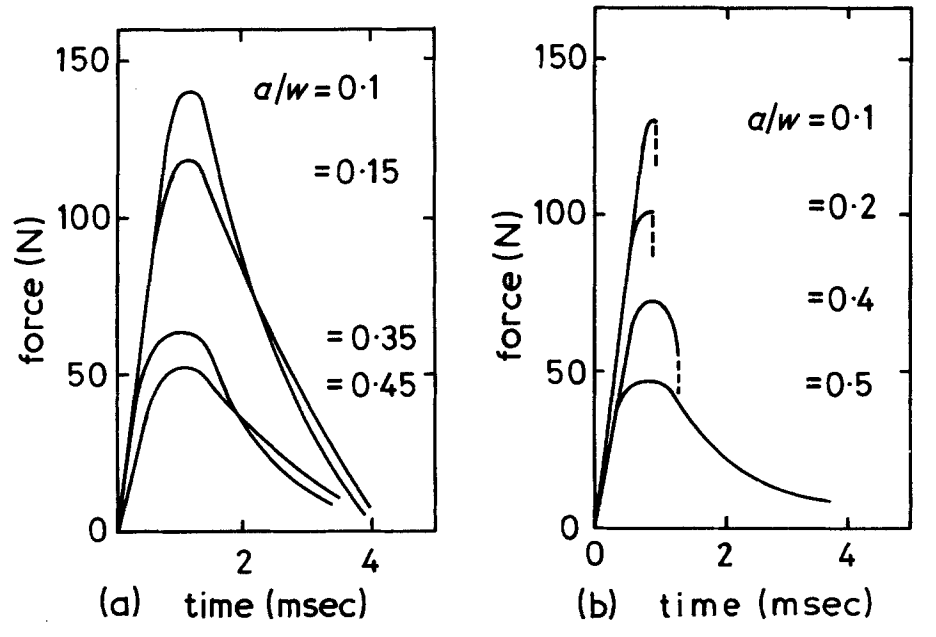


*Figure 6* Load–time curves from instrumented impact at +23° C, $B = 3$ mm, (a) blend 2 and (b) blend 3..

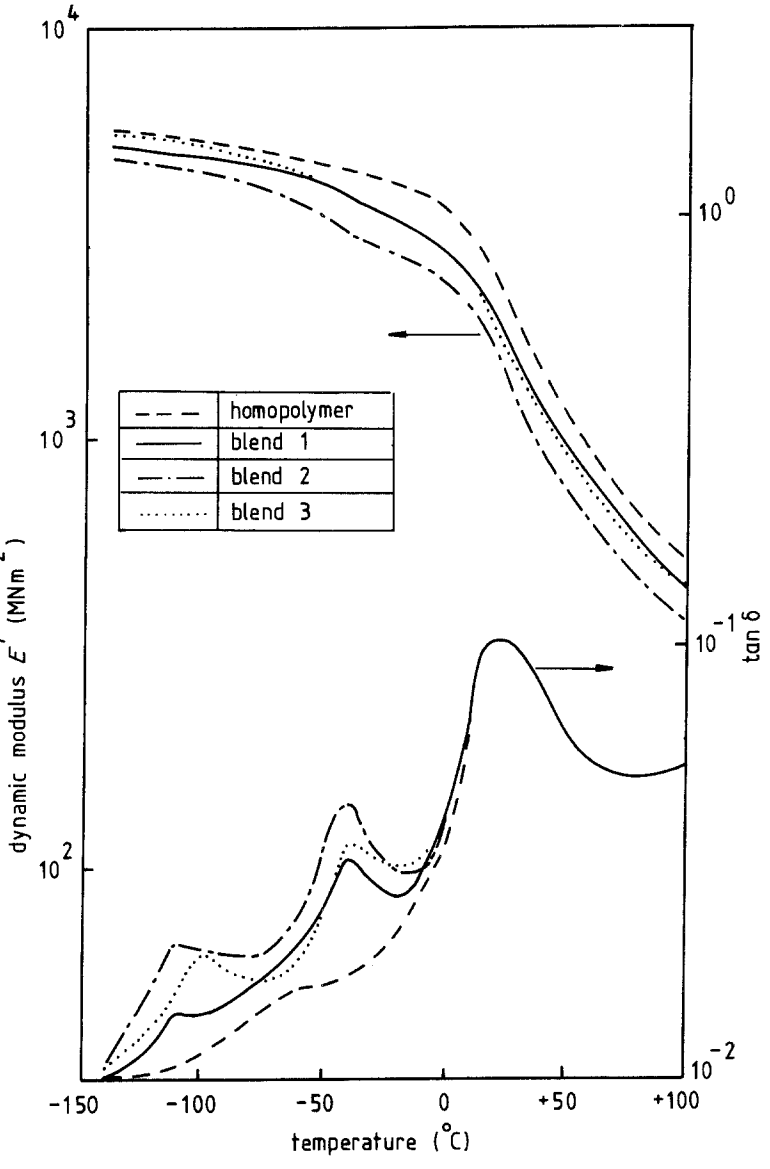


*Figure 7* Dynamic modulus and loss factor as a function of temperature.

## 4.2. Scanning electron microscopy

Samples of each material were soaked in liquid nitrogen and fractured at that temperature and a Jeol JSM-T200 scanning electron microscope was used to study the fracture surfaces. Representative photomicrographs are presented in Fig. 9, and Fig. 9a shows the fractured surface of the homopolymer. The marker bars at the bottom of the micrograph are 10 $\mu$m long, giving an indication of the scale of the surface features. These irregular platelet like features may be due to the interspherulitic cleavage, [18], a description typical of all the matrices examined here. With the introduction of rubber, small holes or lumps begin to appear on the fracture surface, the dimensions of these inclusions are comparable with the separated phase indicated by the optical microscope in DIC, being of the order 1 to 2 $\mu$m. The fracture surface of blend 1 containing 10% rubber is shown in Fig. 9b and here relatively few holes are in evidence, however in Fig. 9c the 20% rubber blend reveals a greatly increased number of second phase particles. Finally in Fig. 9d is shown the fracture surface for blend 3, the 10% rubber/5% HDPE blend and here the effect is similar to the previous blends but there appears to be far more debris on the surface rather than holes.

# 5. Discussion

## 5.1. Fracture mechanics

It has been shown [1] that the toughness measured in bending approximates closely to the plane strain

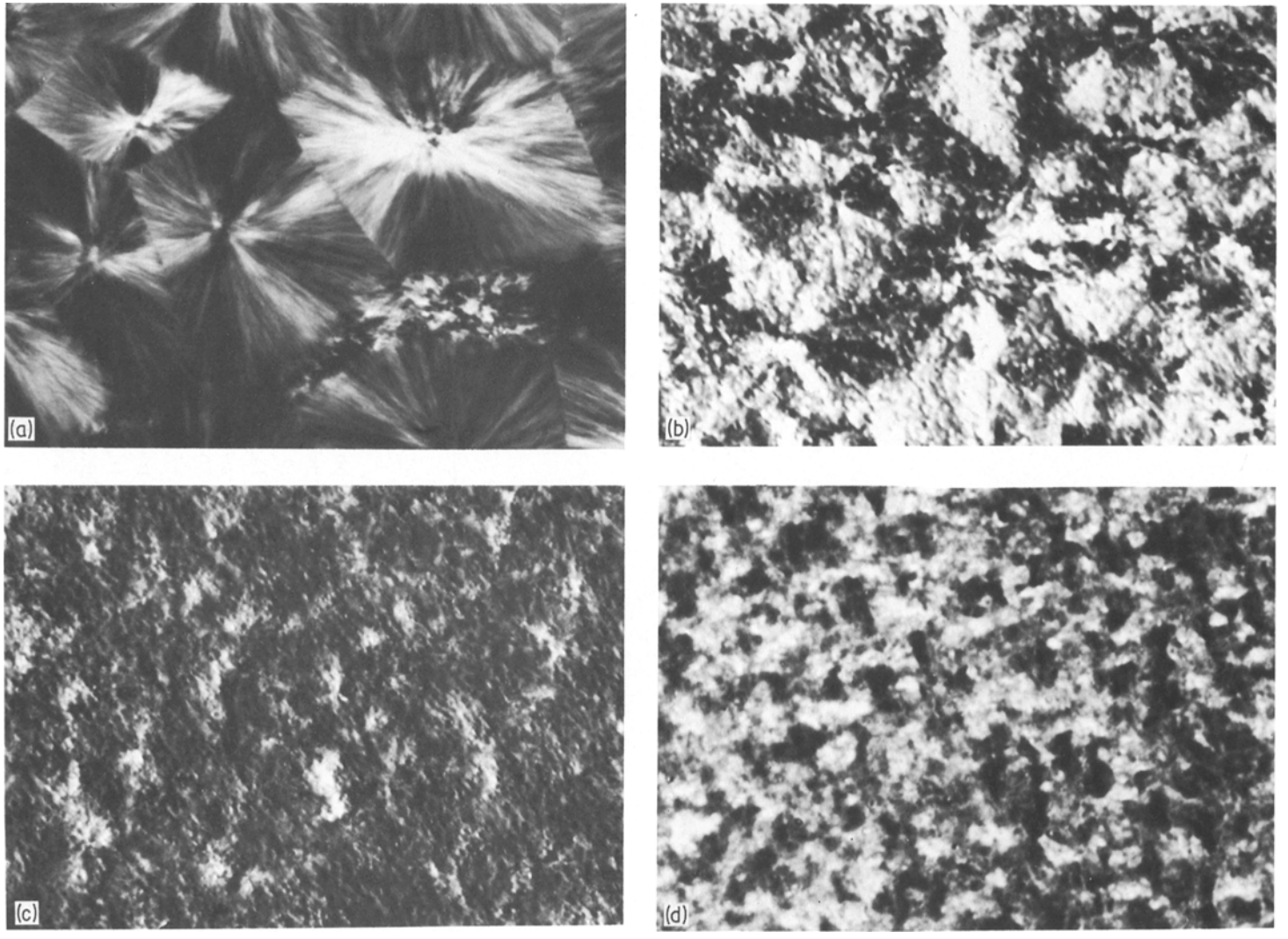


*Figure 8* Structural studies using differential interference contrast (a) homopolymer, (b) blend 1, (c) blend 2 and (d) blend 3.

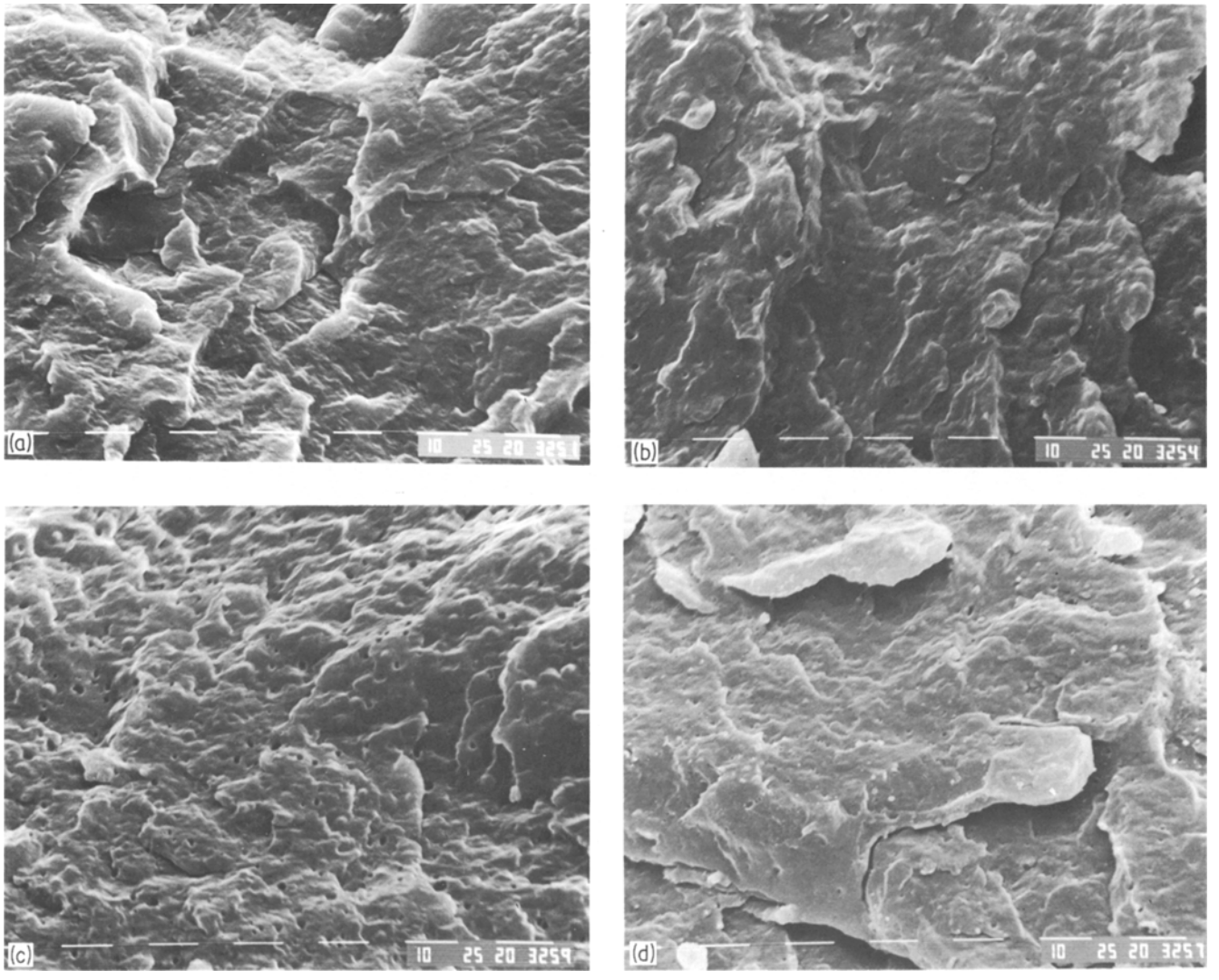


*Figure 9* Scanning electron micrographs of fracture surfaces (a) homopolymer, (b) blend 1, (c) blend 2 and (d) blend 3.

toughness $K_{c1}$, and that SEN tension introduces plane stress effects. The influence of rubber content on the fracture toughness at −60° C measured in SEN bending and tension is shown in Fig. 10. Clearly there is a small effect in bending, the toughness falling off gradually as the proportion of rubber is increased. The addition of 5% HDPE to form blend 3 appears to have the same effect as EPR on the fracture toughness. Conversely, as expected, the toughness measured in SEN tension, $K_c'$, increases steadily with increased rubber fraction, again the addition of HDPE has the same effect as the rubber.

This apparent toughness in tension $K_c'$ has been modelled for polypropylene copolymers [2] by a simple averaging procedure involving the plane strain and plane stress toughness $K_{c1}$ and $K_{c2}$. The relationship is expressed as:

$$K_c' = K_{c1} + \frac{K_{c2}^2}{\pi\sigma_y^2 B}(K_{c2} - K_{c1}) \qquad (3)$$

With the exception of $K_{c2}$ all of the parameters involved have been determined experimentally thus allowing the plane stress toughness to be computed. The results of these computations for

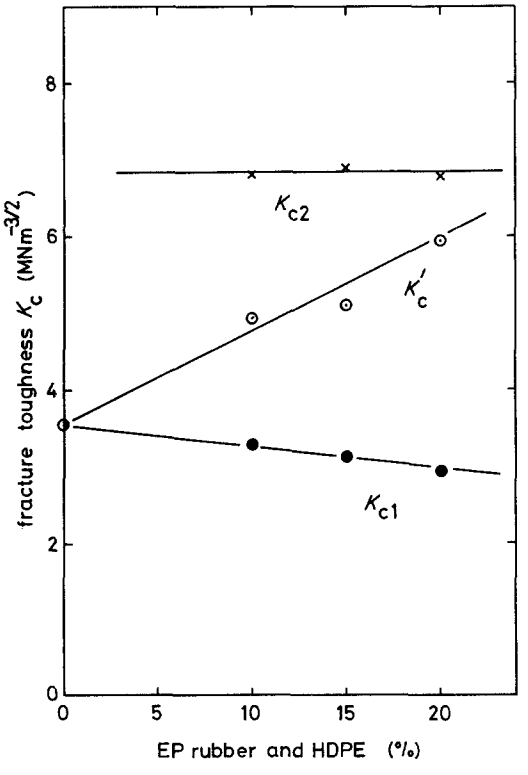


*Figure 10* Fracture toughness as a function of rubber and HDPE content at −60° C.

data at −60° C are shown in Fig. 10, the plane stress toughness proving to be unaffected by rubber content. Indeed the data shown here are very similar to those determined by Fernando and Williams [1, 2] for polypropylene copolymers.

Fernando and Williams [2] noted that the addition of ethylene to the homopolymer caused an initial drop in $K_{c1}$ of some 14%, the toughness subsequently remaining independent of ethylene content. For the blends of this work however, $K_{c1}$ falls monotonically with increasing rubber content as shown in Fig. 10. It is interesting to note that at all temperatues below −40° C the homopolymer proves to be the toughest material in SEN bending. Fig. 11 shows $K_{c1}$ as a function of temperature for the homopolymer and blends, and although the toughness of blend 3 varies somewhat with temperature, on the whole $K_{c1}$ for the blends remains constant for this temperature range. The divergence in toughness between the homopolymer and blends occur at approximately − 40° C, the $T_g$ of the rubber phase which coincides with the $\beta$ transition in ethylene. It may be that these transitions cause embrittlement of the rubber inclusions rendering them less effective as filler particles than the base materials when subject to high constraint.

The temperature dependence of fracture toughness determined in SEN tension and bending for blend 1 is shown in Fig. 12. For the tension experiments the apparent toughness $K_c'$ falls rapidly as the temperature is reduced from −60° C until at approximately −120° C it is equivalent to that determined in bending, $K_{c1}$. This parameter, $K_{c1}$ is constant throughout the measuring temperature range. The plane stress toughness, $K_{c2}$, calculated using Equation 3 also shows a decrease with falling temperature. The toughness of blends 2 and 3 showed a similar temperature dependence to that described for blend 1, and Fernando and Williams [1] noted a similar effect for copolymers.

Surface notch data in this series of tests is somewhat limited, being restricted to a single temperature and notch depth, but variation of the notch width, $b$, allowed examination of its effect on toughness. A similar analysis has been carried out previously on polypropylene copolymers [10] and it was shown that toughness decreased with increasing crack width, and this is also the case here. Table III shows the minimum experimental values of $K_c$ determined using surface notches (large crack width) to be similar to those for SEN

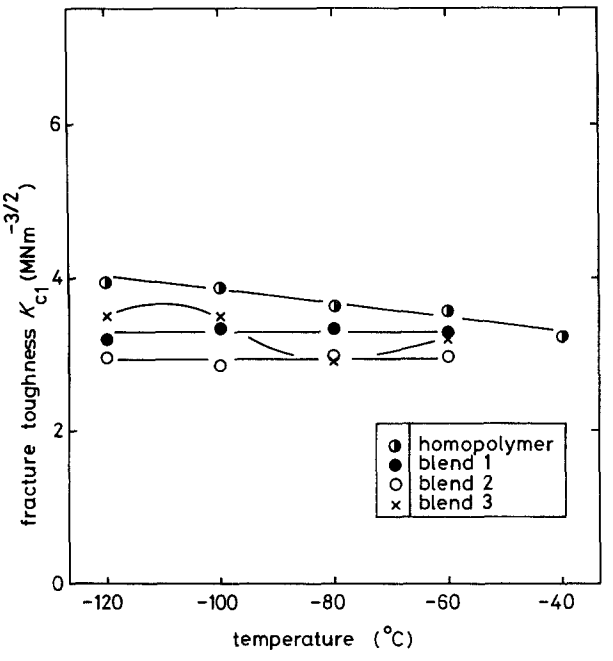


*Figure 11* Fracture toughness determined in SEN bending as a function of temperature.

bending at −80° C, indicating a similar level of constraint for these two experiments.

## 5.2. Impact fracture

The classification of impact failures in various grades of rubber modified polystyrene (HIPS) led to the identification of four modes of failure [19], brittle, semi-brittle, semi-ductile and fully ductile. The least brittle behaviour in this work occurs in the 3 mm thick specimens, and from Figs. 5 and 6 it is clear that these polypropylene based materials at ambient temperature cover a similar spectrum of failure behaviour as HIPS.

The homopolymer behaves in a brittle manner for all thickness and $a/D$ ratios and although blend 1 exhibits slight curvature in the load-deflection graphs of Fig. 5, this is likely to cause a problem only at the highest $a/D$ ratios and for the 3 mm thick specimens. For this impact analysis the majority of specimens have $a/D$ ratios below 0.1 so that problems linked to ductility are likely to be limited to low values of $BD\phi$. The high rubber blend 2 is fully ductile for $a/D$ ratios even as low as 0.1 when the thickness is 3 mm, and also for high $a/D$ ratios for the increased thickness specimens. Even for this material however it is possible to define the impact fracture toughness for these specimens at large $BD\phi$. Blend 3 response is shown in Fig. 6 to be intermediate between that of blends 1 and 2. An explanation for this behaviour has been given previously [4, 20]. In addition to plane stress effects being introduced due to a lack of constraint when specimens are relatively thin, there is also an increasing strain rate effect with increased $a/D$ ratio. At high $a/D$ the loading time to failure is significantly reduced causing heat

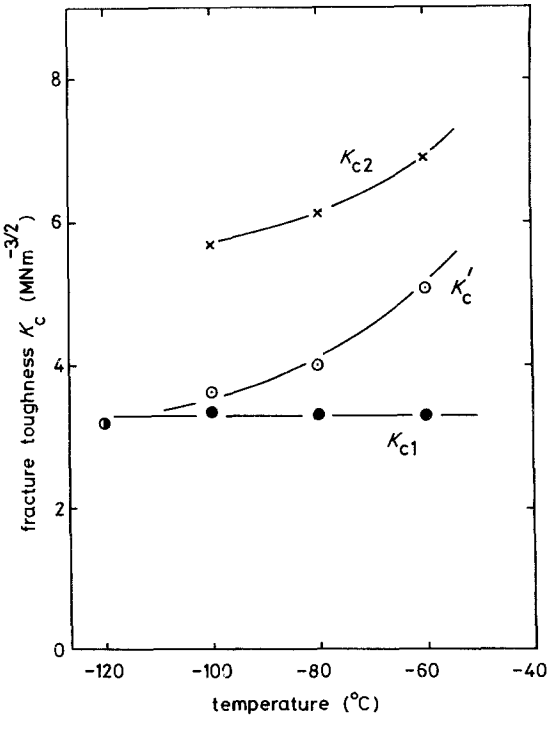


*Figure 12* Fracture toughness as a function of temperature for blend 1 in tension and bending.

generated at the running crack tip to be contained within a small volume of material. This results in adiabatic heating of the crack tip area and consequent blunting of the crack so that additional energy is required to break the specimen. Specimens with shorter cracks have a longer loading time associated with their failure, and any heat generated during fracture is dissipated isothermally. The fracture energy under these circumstances is a true reflection of brittle behaviour from which the impact fracture toughness $G_c$ may be determined.

Considering the worst cases, when the thickness $B$ is 3 mm, impact data for the blends is plotted in Fig. 13. Blend 1 indicates a linear relationship between the fracture energy and $BD\phi$ across the full range of $\phi$. As expected blends 2 and 3 suffer from the effects of crack tip blunting with greatly increased recorded energy to failure at low $\phi$ values. At higher $\phi$ however the relationship between $\phi$ and fracture energy becomes linear, and it is the slope of the line drawn through these data points which defines the impact fracture toughness $G_c$ recorded in Table IV.

The effects of decreased loading time are further

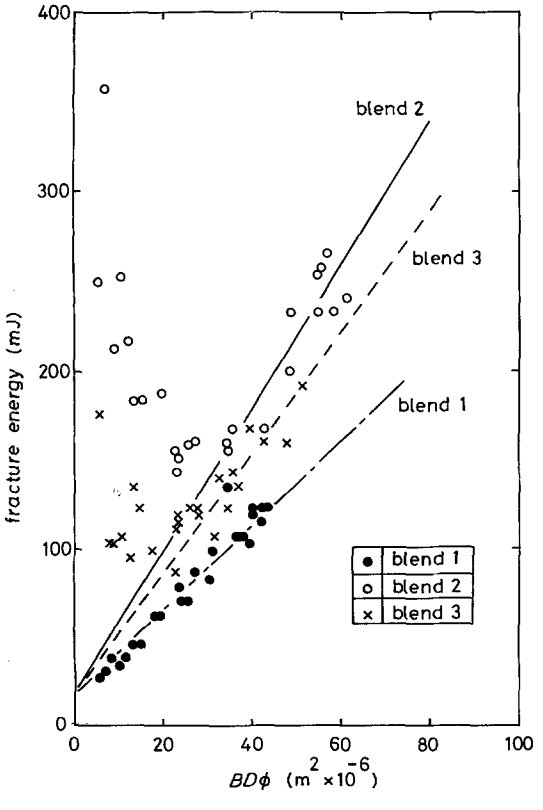


*Figure 13* Impact fracture energy as a function of $BD\phi$ for the blends at +23° C for $B = 3$ mm.

demonstrated in Fig. 14, where the apparent toughness $G_b$ for each specimen is plotted as a function of calculated loading time, here the loading time $t$ is given by [4]:

$$t = \frac{D}{V}\left(\frac{G_c}{ED}\right)^{1/2}\left[\frac{3L}{D}\phi(Y^2x)^{1/2}\right]. \quad (4)$$

The homopolymer and blend 1 which are relatively brittle at all values of $\phi$ do show some scatter but change little with decreasing loading time. The homopolymer does however show a small increase in apparent toughness above its base value of 1.2 kJ m$^{-2}$ as the loading time falls below 0.2 msec. Blend 1 never actually falls below this loading time and is fairly consistent about its own base value of 2.1 kJ m$^{-2}$ for blends 2 and 3 the effect of short loading times is dramatic. Blend 2 has a critical loading time of around 0.5 msec and blend 3 slightly lower at 0.4 msec, below these loading times the apparent toughness increases rapidly to values as high as 49 kJ m$^{-2}$.

This effect has been modelled previously [20]. Using a similar approach here it is possible to define the time scale $t_1$ for this rapid increase in toughness in terms of the apparent ($G_b$) and base ($G_c$) toughnesses and a parameter $N$ which incorporates the yield stress and strain and fracture stress, such that:

$$\left(\frac{G_b}{G_c} - \frac{1}{2}\right)^{1/2} = N^{-1}\left[1 - \left(\frac{t_1}{t}\right)^{1/2}\right]. \quad (5)$$

$N$ and $t_1$ may be determined graphically as shown in Fig. 15 for blend 2. These experimental data and those for the other materials are collected together in Table V. The determination of $N$ and $t_1$ allows the computation of theoretical curves of $G_b$ as a function of loading time and these are shown in Fig. 14. The correlation with experimental data for blends 2 and 3 is good and it might be expected that the homopolymer and blend 1 would give similar agreement if tested at slightly higher rates. The time $t$ at which the curves join the base toughness line for each material is also recorded in Table V and indicates the loading time at which thermal blunting begins. Calculation of $t_1$ and $t_0$ from the base toughness $G_c$, softening temperature $T_s$, test temperature $T_0$ and material parameters including the density $\rho$, specific heat $c$ and thermal conductivity $k$, using the relationships [20]:

$$t_1 = G_c^2/(T_s - T_0)^2\pi\rho ck \quad (6)$$

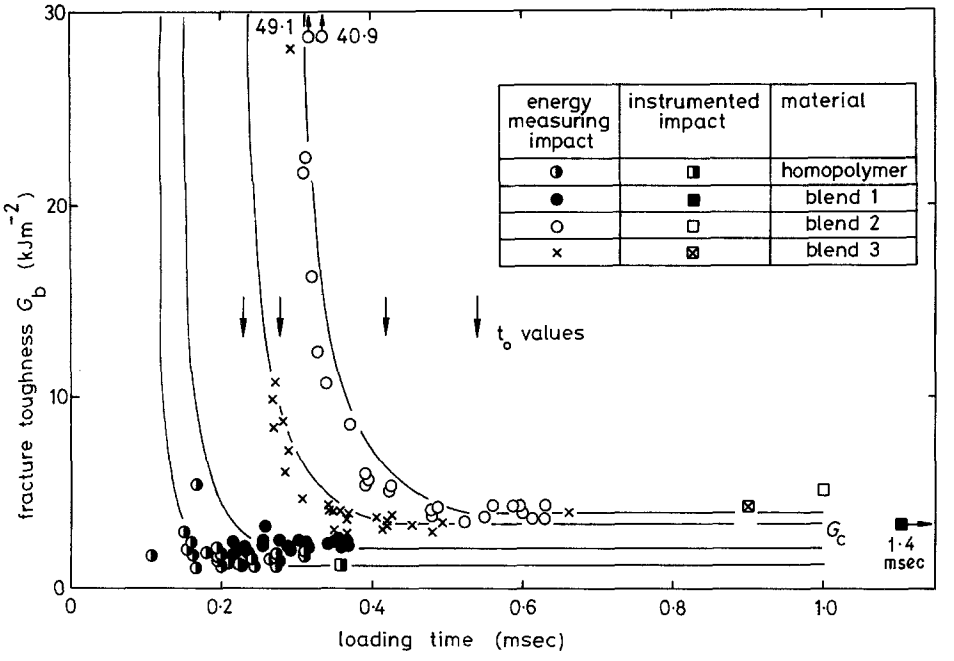


*Figure 14* Impact fracture toughness as a function of loading time for $B = 3$ mm.

and

$$t_0/t_1 = [1-(2)^{1/2}N]^{-2} \quad (7)$$

are also recorded in Table V, together with the assumed values of $T_s$, $\rho$, $c$ and $k$. It will be noted that for these calculations the parameters $\pi\rho ck$ relevant to polypropylene were used only for the homopolymer. For all blends it was thought more correct to use values determined for the rubber on the grounds that any temperature rise in the material due to fast fracture would have more effect in the rubber regions. When these calculated loading times are compared with those determined experimentally extremely precise agreement is found for the homopolymer and quite close correlation for the blends. These slight deviations in critical loading time indicate variations in the temperature rise at fracture, the computed temperature increases being recorded in Table V.

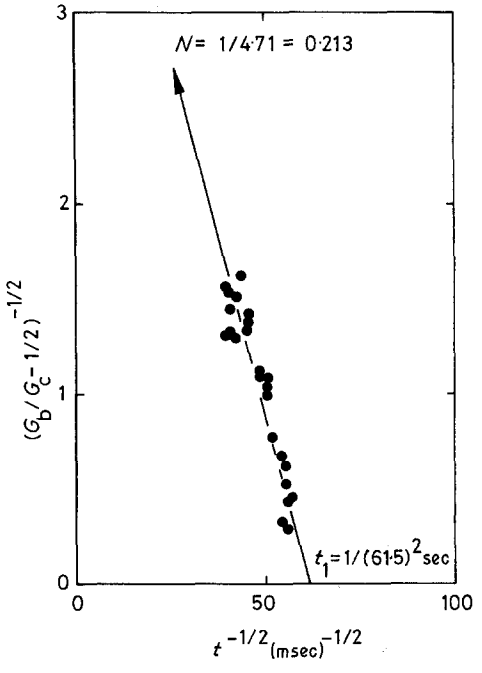


*Figure 15* The determination of $N$ and $t_1$ for blend 2.

The base impact toughnesses determined at long loading time and recorded in Table IV, are plotted as a function of toughening agent for 3 mm thick specimens in Fig. 16. The effect on blending rubber and HDPE is obvious, a reasonably linear relationship being described between $G_c$ and the proportion of toughening agent, HDPE having a similar effect to that of the rubber. Using the relationship [21]:

$$K_c^2 = EG_c \quad (8)$$

the elastic modulus (in this case that determined dynamically) may be used to express the impact strain energy release rate as an equivalent stress intensity factor $K_c$. This has been done and the results are shown in Table IV together with the toughness data obtained using the instrumented pendulum. The agreement between the calculated

TABLE V Data for the limiting loading time in impact

| Material | Experimental | | | Computed | | |
|---|---|---|---|---|---|---|
| | $G_c$ (kJ m$^{-2}$) | $t_1$ (msec) | $t_0$ (msec) | $t_1$ (msec) | $t_0$ (msec) | $T_c$ (°C) |
| Homopolymer | 1.2 | 0.113 | 0.23 | 0.113 | 0.23 | 160 |
| Blend 1 | 2.1 | 0 137 | 0.28 | 0.103 | 0.21 | 141 |
| Blend 2 | 4.0 | 0.264 | 0.53 | 0.372 | 0.76 | 186 |
| Blend 3 | 3.4 | 0.207 | 0.42 | 0.269 | 0.55 | 180 |

$N = 0.213$.
Assumed values: softening temperature $T_s = 160°$ C.
$\pi\rho ck$ (homopolymer) $= 0.65 \times 10^6$ J$^2$ (sm$^4$K$^2$)$^{-1}$.
$\pi\rho ck$ (rubber) $= 2.19 \times 10^6$ J$^2$ (sm$^4$K$^2$)$^{-1}$.
(obtained from G. W. C. Kaye, T. H. Laby, Tables of Physical and Chemical constants, Longmans, 1973).

toughness data and those determined experimentally is quite good. If on the other hand the stress intensity factor $K_c$ determined using the instrumented pendulum is converted to the equivalent $G_c$, using the appropriate modulus, a comparison may be made with the apparent toughness determined from the energy measuring impact test. Traces from the instrumented impact tests gave accurate indicators of the loading time to failure, as shown in Figs. 5 and 6, so that the equivalent $G_c$ could be plotted as a function of loading time. The data points obtained from the 3 mm thick specimens have been added to Fig. 14, these $G_c$ values being very similar to the base $G_c$ levels determined by the energy measuring system at low $a/D$ ratios. The reason for this is clearly that the instrumented machine operates at a lower striker velocity and gives data at longer loading times, so that the $G_c$ measured is always the base value.

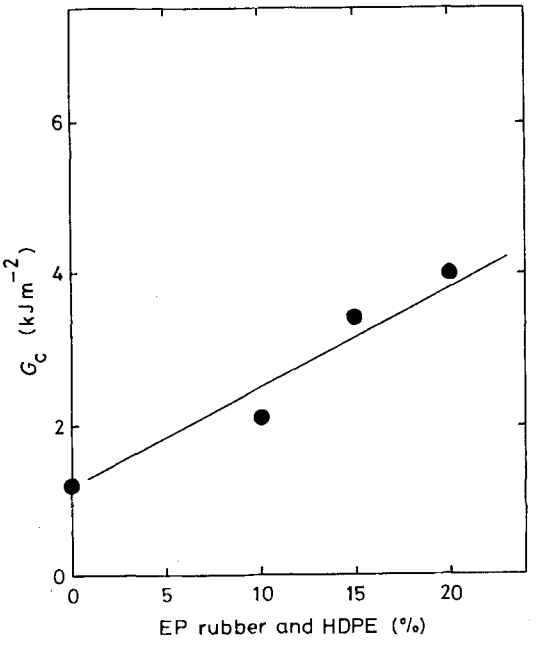


*Figure 16* Impact fracture toughness as a function of rubber and HDPE content at +23° C, $B = 3$ mm.

## 6. Conclusions

A number of experiments have been carried out on a range of polypropylene/EPR and HDPE blends in order to define their properties and to draw comparisons with copolymers of propylene and ethylene which were the subject of previous work [1, 2, 5]. At −60° C the fracture behaviour of the homopolymer of this study is properly described by linear elastic fracture mechanics, and the mean of plane strain toughness measurements at −60° C defines this toughness as 3.85 MN m$^{-3/2}$. This value falls between the two values of the previous work [1, 2] which at 4.7 and 3.3 MN m$^{-3/2}$ demonstrate that the toughness of different homopolymer materials vary widely. This is likely to have a systematic effect on the toughness of blends or copolymer materials dependent upon homopolymer properties. It follows that direct comparison of the results is probably not valid and has not been attempted. It could however be expected that the effects of blending EPR or addition of ethylene as a copolymer might well be similar.

It was observed previously [2] that the toughness appeared to fall immediately on the addition of ethylene, to a constant value some 14% below that of the homopolymer. This led to the proposition [5] that the effect could be due to head-to-head linkages in the polymer chains. This thesis does not appear to be applicable to the work carried out here, since although it is true that the plane strain toughness falls with the addition of EPR, the reduction in toughness is monotonic with increasing rubber or HDPE content. This might however be expected since on blending there

is no molecular linkage between the propylene and the rubber as there is in a copolymer.

The apparent toughness $K_c'$ as measured in the single edge notch mode increased with rubber content as was found to be the case with increased ethylene content in the copolymers. The calculated plane stress toughness $K_{c2}$ remained constant at a similar value to that found in the previous work [2]. With changing temperature, although there is some scatter, the plane strain toughness remains reasonably constant, the homopolymer proving to be the toughest material at each test temperature. When tested in the single edge notch mode the apparent $K_c'$ of the blends was found to increase with increasing temperature, slowly between $-100$ and $-80^\circ$ C but more rapidly from $-80$ to $-60^\circ$ C. This behaviour was also very similar to that of the copolymer materials investigated previously.

It was shown previously [2], that thermal treatment of the homopolymer and copolymers had a significant effect on toughness due to changes in spherulite size. This cannot however be put forward as a reason for differences in unheat-treated homopolymer toughness as the spherulite size was similar in each case. What has been shown by morphological studies is that the rubber of the blends and the ethylene of the copolymers aggregates in very similar second phase particles. So that it is perhaps not surprising that the properties of these materials are quite similar.

In impact at $+23^\circ$ C good agreement was found between results from energy measuring and instrumented machines at long loading times. It has been shown however that below a critical loading time the toughness increases dramatically due to a thermal blunting mechanism described in detail elsewhere [4, 20]. The timescale of this thermal blunting is quite accurately defined by the previously proposed theory [20] in terms of the materials thermal properties, toughness and softening temperature. The increase in toughness with decreasing loading time was also found to be predictable.

The notch blunting parameter $N$ was found to have a constant value of 0.213 for these polypropylene based materials, and when coupled with a typical yield strain of about 4% results in an effective constraint factor at the crack tip [20] of 1.5. Such a low value of constraint factor (PMMA = 4, HDPE = 10) could be interpreted in terms of the known notch sensitivity of polypropylene in impact at and below ambient temperatures. Such a conclusion lends support to the proposition [20] that $N$ could be useful in the derivation of a generalized ductile–brittle criterion.

Impact toughness data from the instrumented impact machine correlated well with long loading time results from the energy measuring system, due to the relatively low impact velocity of the instrumented pendulum prohibiting any thermal effects. At long loading times the impact toughness was found to be directly proportional to the toughening agent content of the polymer.

## Acknowledgements

It is with pleasure that the authors acknowledge Montepolimeri S.p.A. for permission to publish this work and Dr P. Prentice for interesting and useful discussions.

## References

1. P. L. FERNANDO and J. G. WILLIAMS, *Polym. Eng. Sci.* **20** (1980) 215.
2. *Idem, ibid.* **21** (1981) 1003.
3. M. K. V. CHAN and J. G. WILLIAMS, *ibid.* **21** (1981) 1019.
4. J. M. HODGKINSON and J. G. WILLIAMS, in Proceedings of the Conference on Mechanical Properties of Materials at High Strain Rates, Oxford, March 1979, Institute of Physics Conference Series No. 47 (Institute of Physics, Bristol, 1980) p. 233.
5. P. PRENTICE and J. G. WILLIAMS, *Plast. Rubber Process. Appl.* **2** (1982) 27.
6. P. PRENTICE, *Polymer* **23** (1982) 1189.
7. F. C. STEHLING, T. HUFF, C. S. SPEED and G. WISSLER, *J. Appl. Polym. Sci.* **26** (1981) 2693.
8. J. KARGER-KOCSIS and V. N. KULEZNEV, *Polymer* **23** (1982) 699.
9. P. I. VINCENT, *ibid.* **15** (1974) 111.
10. M. KISBENYI, M. W. BIRCH, J. M. HODGKINSON and J. G. WILLIAMS, *ibid.* **20** (1979) 1289.
11. P. L. FERNANDO, PhD thesis, University of London (1980).
12. W. F. BROWN and J. E. SRAWLEY, ASTM STP 410 (American Society of Testing and Materials, Philadelphia, 1966).
13. E. PLATI and J. G. WILLIAMS, *Polymer* **16** (1975) 915.
14. G. P. MARSHALL, J. G. WILLIAMS and C. E. TURNER, *J. Mater. Sci.* **8** (1973) 949.
15. T. CASIRAGHI, *Polym. Eng. Sci.* **18** (1978) 833.
16. T. CASIRAGHI and A. SAVADORI, *Plast. Rubber: Mater. Appl.* (1980) 1.
17. W. LANG, Reprint S-41-210-2-5-e, Carl Zeiss, Oberkochen, West Germany.
18. K. FRIEDRICH, *Prog. Colloid Polym. Sci.* **66** (1979) 299.
19. K. NIKPUR and J. G. WILLIAMS, *J. Mater. Sci.* **14** (1979) 467.

20. J. G. WILLIAMS and J. M. HODGKINSON, *Proc. Roy. Soc. Lond.* **A375** (1981) 231.
21. G. R. IRWIN, *Appl. Mater. Res.* **3** (1964) 65.

*Received 11 October*
*and accepted 20 December 1982*